



Teriflunomide Treatment of Multiple Sclerosis Selectively Modulates CD8 Memory T Cells

Gaëlle Tilly¹, Marion Cadoux¹, Alexandra Garcia¹, Jérémy Morille¹,
Sandrine Wiertelowski^{1,2}, Claire Pecqueur³, Sophie Brouard¹,
David Laplaud^{1,2} and Nicolas Degauque^{1*}

¹ Université de Nantes, CHU Nantes, Inserm, Centre de Recherche en Transplantation et Immunologie, UMR 1064, ITUN, Nantes, France, ² CHU Nantes, Service de Neurologie, CRC-SEP, CIC1413, Nantes, France, ³ Université de Nantes, CRCINA, INSERM, CNRS, Nantes, France

OPEN ACCESS

Edited by:

Marcello Moccia,
University of Naples Federico II, Italy

Reviewed by:

Johann Sellner,
Landesklinikum Mistlbach-
Gänserndorf, Austria
Hartmut Wekerle,
Max-Planck-Gesellschaft (MPG),
Germany

*Correspondence:

Nicolas Degauque
nicolas.degauque@univ-nantes.fr

Specialty section:

This article was submitted to
Multiple Sclerosis
and Neuroimmunology,
a section of the journal
Frontiers in Immunology

Received: 24 June 2021

Accepted: 10 September 2021

Published: 05 October 2021

Citation:

Tilly G, Cadoux M, Garcia A, Morille J,
Wiertelowski S, Pecqueur C, Brouard S,
Laplaud D and Degauque N (2021)
Teriflunomide Treatment of
Multiple Sclerosis Selectively
Modulates CD8 Memory T Cells.
Front. Immunol. 12:730342.
doi: 10.3389/fimmu.2021.730342

Background and Objectives: Inhibition of *de novo* pyrimidine synthesis in proliferating T and B lymphocytes by teriflunomide, a pharmacological inhibitor of dihydroorotate dehydrogenase (DHODH), has been shown to be an effective therapy to treat patients with MS in placebo-controlled phase 3 trials. Nevertheless, the underlying mechanism contributing to the efficacy of DHODH inhibition has been only partially elucidated. Here, we aimed to determine the impact of teriflunomide on the immune compartment in a longitudinal high-dimensional follow-up of patients with relapse-remitting MS (RRMS) treated with teriflunomide.

Methods: High-dimensional spectral flow cytometry was used to analyze the phenotype and the function of innate and adaptive immune system of patients with RRMS before and 12 months after teriflunomide treatment. In addition, we assessed the impact of teriflunomide on the migration of memory CD8 T cells in patients with RRMS, and we defined patient immune metabolic profiles.

Results: We found that 12 months of treatment with teriflunomide in patients with RRMS does not affect the B cell or CD4 T cell compartments, including regulatory T_{REG} follicular helper T_{FH} cell and helper T_H cell subsets. In contrast, we observed a specific impact of teriflunomide on the CD8 T cell compartment, which was characterized by decreased homeostatic proliferation and reduced production of TNF α and IFN γ . Furthermore, we showed that DHODH inhibition also had a negative impact on the migratory velocity of memory CD8 T cells in patients with RRMS. Finally, we showed that the susceptibility of memory CD8 T cells to DHODH inhibition was not related to impaired metabolism.

Discussion: Overall, these findings demonstrate that the clinical efficacy of teriflunomide results partially in the specific susceptibility of memory CD8 T cells to DHODH inhibition in patients with RRMS and strengthens active roles for these T cells in the pathophysiological process of MS.

Keywords: multiple sclerosis, teriflunomide, CD8 T cells, CD4 T cells, migration, memory T cells

INTRODUCTION

The selective and reversible inhibition of dihydroorotate dehydrogenase (DHODH), a key mitochondrial enzyme in the *de novo* pyrimidine synthesis pathway, by teriflunomide has been shown to be a safe and effective strategy to treat patients with multiple sclerosis (MS). The results obtained from phase 3 clinical trials demonstrated that patients with MS treated with teriflunomide show a significant reduction in disability progression and relapse rate and lower magnetic resonance imaging evidence of disease activity (1, 2). The primary mechanism of action explaining the success of DHODH inhibition is the suppression of stimulated T and B cell proliferation (3–5) by inducing metabolic stress in metabolically proliferating lymphocytes. The addition of exogenous uridine can overcome the antiproliferative effect of teriflunomide (6), and the selective effect on activated T and B cells is partially explained by the activation of the salvage pathway in resting cells to meet their pyrimidine needs (7, 8). Nevertheless, the mechanism of immune system modulation induced by teriflunomide remains unclear, with contradictory results reported. A decrease in only the frequency of CD45RA⁺ effector memory (TEMRA) CD4 T cells and plasmablasts has been reported for patients with MS after 6 months of treatment, while the frequency of other immune cells, including CD8 T cells, remained similar before and after DHODH inhibition (9). The production of proinflammatory cytokines (IFN γ , TNF α and IL-17) by CD4 T cells was not modified after 6 months of treatment (9). In contrast, another study reported a specific decrease in IFN γ , TNF α and IL-17 in both the CD4 T_H1 and CD8 T cell compartments (10). High-affinity CD4 and CD8 T cell clones have been shown to be more susceptible to DHODH inhibition, and individual T cell clones are eliminated from the TCR V β repertoire of patients with MS within weeks of initial teriflunomide treatment (10). The contradiction regarding the impact of DHODH inhibition on the immune system has prompted the need to further characterize the immune system of MS patients, particularly with a longitudinal paired analysis and high-dimensional approach.

Immunopathology of MS has been widely studied, and based on models of experimental autoimmune encephalomyelitis, the concept of MS as an autoimmune disease mediated by CD4 T_H1/T_H17 cells specific to autoantigens of the CNS (11) has emerged. As major attention has been given to the CD4 T cell compartment in the analysis of MS patients, the impact of DHODH inhibition on CD8 T cells has not been carefully investigated. Nevertheless, our results and other accumulated

evidence suggest a major role of CD8 T cells. Active lesions are infiltrated mainly by CD8 T cells that are in close proximity to oligodendrocytes and demyelinating axons (12, 13). CD8 T cell clones are shared between CSF and active white matter lesions (14, 15) and are also present in peripheral blood (15). Moreover, the involvement of DHODH in the key process of CD8 T cell migration has not yet been investigated, although the recirculation of memory T cells is a central process in the establishment of the immune response involving the localization of memory CD8 T cells in secondary lymphoid organs and nonlymphoid tissues.

In this study, we investigated the impact of DHODH inhibition in patients with relapse-remitting MS (RRMS) before and 12 months after treatment using high-dimensional flow cytometry to characterize the immune system as a whole. We demonstrated that DHODH inhibition had no impact on the CD4 T compartment without any modification in the frequency of CD4 T helper cells, CD4 T follicular cells or CD4 regulatory T cells or in the function of CD4 T helper and CD4 regulatory cells. In contrast, we showed that DHODH inhibition impacted the proliferation of CD8 T cells and the production of proinflammatory cytokines through effector memory (EM) and TEMRA CD8 T cells and their migratory properties. Finally, we demonstrated that the susceptibility of memory CD8 T cells to DHODH inhibition was not related to impaired metabolism.

METHODS

Standard Protocol Approvals, Registrations, and Patient Consents

Patients included in the study suffered all from relapsing-remitting MS as defined by the revised MacDonald criteria published in 2005, and the demographic and clinical characteristics are shown in **Table 1**. Twelve out of 15 MS patients were naïve of any treatment at the time of teriflunomide start. The three other patients were previously treated with an immunomodulatory treatment (Interferon beta, dimethyl-fumarate) that was stopped at least three months before Teriflunomide initiation. Finally, Teriflunomide was started at least 6 months after a relapse for all the patients. The University Hospital Committee and the Committee for the Protection of Patients from Biological Risks approved the study (ABM PFS13-003 “Collection sclérose en plaques”), and all patients were recruited after obtaining informed signed consent.

Blood Samples

PBMCs were separated from blood samples collected in EDTA tubes on a Ficoll gradient layer according to the manufacturer's recommendations and were frozen in autologous serum with 10% DMSO. PBMCs were then thawed in CTL wash supplemented with benzonase (10 U/mL).

Reagents

The antibodies used for flow cytometry analyses and key reagents are listed in **Supplementary Tables 1 and 2**.

Abbreviations: 2-DG, 2-deoxyglucose (2-DG); CPD, cell proliferation dye eFluor450; DHODH, dihydroorotate dehydrogenase; ECAR, extracellular acidification rate; EM, effector memory; FlowSOM, flow cytometry self-organizing map; GLUT1, glucose transporter 1 GLUT1; MFI, mean fluorescence intensity; MMP, mitochondrial membrane potential; MS, multiple sclerosis; OCR, oxygen consumption rate; opt-SNE, optimized t-distributed stochastic neighbor embedding; PBMC, peripheral blood mononuclear cells; PPMS, primary progressive; TEMRA, CD45RA⁺ effector memory; T_{FH} cell, T follicular helper cell; T_H cell, T helper cell; T_{REG}, regulatory T cell; SPMS, secondary progressive; RRMS, relapse-remitting MS.

TABLE 1 | Demographical and clinical characteristics of the patients at sampling.

Form of the disease (%)	Sex ratio	Disease duration [years, median (IQR _{25-75%})]	Time between last flare and treatment initiation [months, median (IQR _{25-75%})]	Age [years, median (IQR _{25-75%})]	EDSS [median (IQR _{25-75%})]	Sampling at flare (Y/N; n)	Previous treatment (Y/N; n)
RR 100%	5 M/ 10 W	3.00 [0.17 – 17.00]	30 [15 – 48]	39.00 [31.00 – 44.00]	0.50 [0.00 – 1.25]	13/2	12/15

CD8 T Cell Isolation and FACS-Sorting of CD8 T Cell Subsets

PBMCs were cultured overnight in complete RPMI medium supplemented with 10% FCS, 100 U/mL penicillin and 100 U/mL streptomycin. CD8 T cells were purified using a human REAlease CD8 MicroBead kit. Naïve (CD45RA⁺CCR7⁺), EM (CD45RA⁻CCR7⁻) and TEMRA (CD45RA⁺CCR7⁻) CD3⁺CD8⁺ cells were sorted from PBMCs by FACS (FACS Aria, BD Biosciences; the purity was greater than 95%).

Immune Profiling by Spectral Flow Cytometry

Two million PBMCs were either directly stained with the “T cell panel” or stimulated with PMA (50 ng/mL) and calcium ionophore (500 ng/mL) for 3.5 h in the presence of brefeldin A (5 µg/mL) before being stained with the “functional panel” (i.e., IL-10, IL-13, IL-17, IFN γ , TNF α). PBMCs were analyzed using an Aurora 5-laser spectral flow cytometer (Cytek). After individual titration of each antibody, a deconvolution matrix was set up according to Cytek recommendations. Quality control procedure was performed prior each data acquisition according to Cytek recommendations.

High-Dimensional Data Analysis of Flow Cytometry Data

Supervised and unsupervised (optSNE and FlowSOM) analyses were performed on OMIQ (<https://www.omiq.ai/>). FCS files were first cleaned using FlowCut (16) and by gating on CD45⁺Singlet⁺LiveDead⁻. Non-naïve CD4 T cells and non-naïve CD8 T cells were analyzed separately. optSNE analysis was performed using equal amounts of samples comprising 1x10⁵ non-naïve CD4 T cells or 5x10⁴ non-naïve CD8 T cells obtained from each FCS pool, with 1000 iterations, a perplexity of 30, and a theta value of 0.5. For the non-naïve CD4 T cells, the expression of the following markers was measured CCR6, CXCR3, CCR4, CD161, CXCR5 and CD28. For the non-naïve CD8 T cells, the expression of the following markers was measured: CCR6, CXCR3, CCR4, CD161, CXCR5 and CD28. For non-naïve CD8 T cells, the expression of the following markers was measured: CD161, CD69, CXCR3, CD57, CD45RA, CD152, CXCR5, CD137, PD-1, TIGIT, CD39, CD194, CCR7, CD49a, TIM3, CD27, LAG3, CD28, KI-67, CD25, CD127, CD73 and CCR6. The resulting optSNE maps were fed into the FlowSOM clustering algorithm (17). For each cell subset, a new self-organizing map (SOM) was generated using hierarchical consensus clustering on the tSNE axes. For each SOM, 12 and 20 metaclusters were identified for non-naïve CD4 T cells and for non-naïve CD8 T cells, respectively.

Metabolic Assays

After FACS sorting, purified CD8 T cell subsets were cultured overnight in TexMACS buffer at 37°C and 5% CO₂. The oxygen consumption rate (OCR) and extracellular acidification rate (ECAR) were measured using 4x10⁵ or 2.5x10⁵ purified CD8 T cell subsets and Seahorse XF24 or XF96 analyzers, respectively. The assay was performed in Seahorse XF-base medium supplemented with 10 mM glucose, 2 mM glutamine, and 1 mM pyruvate. A mitochondrial stress assay was performed by successively adding oligomycin (1.5 µM), CCCP (1 µM), and anti-mycin A + rotenone (1 µM each). To assess the OCR and ECAR upon polyclonal stimulation, PMA (50 ng/mL) and ionomycin (500 ng/mL) were added 75' after the start of the experiment. 2-DG (250 mM) was added before stimulation with PMA-Iono.

Quantification of Mitochondrial and Mitochondrial Membrane Potential (MMP)

MitoTracker green and MitoTracker red were used to quantify mitochondria and to assess the MMP, respectively. PBMCs were first incubated with 100 nM MitoTracker green or MitoTracker red for 30' at 37°C and 5% CO₂, and then, the cells were stained using anti-CD3, anti-CD8, anti-CD45RA, and anti-CD28 antibodies. The samples were immediately analyzed with an LSRII flow cytometer.

Glucose Transporter Expression

PBMCs were stimulated overnight or not with aCD3 (2 µg/mL) and then stained using anti-CD3, anti-CD8, anti-CD45RA, anti-CD28 and anti-Glut1 antibodies according to the manufacturer's instructions. GLUT1 expression in CD8 T cell subsets was assessed according to mean fluorescence intensity (MFI).

Activation and Proliferation

CD8 T cell isolation or FACS-sorted CD8 T cell subsets were plated in 96-U bottom plates coated with anti-CD3 mAb (2 µg/mL) and cultured for 1–5 days in RPMI complete medium with IL-15 (10 ng/mL) or anti-CD28 mAb (2 µg/mL). Proliferation was monitored using diluted cell proliferation dye eFluor450 (CPD) and assessed according to the frequency of CPD^{low} cells on days 4 and 6. After culturing overnight, activation (CD25 and CD69) and proinflammatory cytokine production (TNF α and IFN γ) of the CD8 T cell subset was determined by cytometry. Teriflunomide (100 µM), uridine (50 µM) and 2-DG (10 mM) were added as indicated.

Cell Migration Assessment Using Time Lapse Microscopy

TEMRA (CD45RA⁺CCR7⁻) and EM (CD45RA⁻CCR7⁻) CD3⁺CD8⁺ cells obtained from MS patients were sorted by

FACS and cultured overnight in complete RPMI medium supplemented with IL-15 (2 ng/ml). CD8 T cell subsets stained with the cytosolic Ca²⁺ indicator Fura-2 AM probe (1 µg/mL for 45 min at room temperature) were seeded on a confluent monolayer of primary Human Dermal Microvascular Endothelial [HDMECs that have been previously and widely used as a good model for the *in vitro* study of inflammatory responses (18)] activated for 24 h with TNFα (100 U/ml) in µ-Slide 8 wells. Teriflunomide (100 µM) or DMSO (negative control) was added after 20 min of cell migration. Cell migration was tracked by time-lapse microscopy through a 20× objective of a Leica DMI 6000B microscope equipped with MetaMorph[®] software (Molecular Devices), and 120 sequential images were captured in 20-second intervals. The migration paths of individual cells were determined with ImageJ software, TrackMate-extras plugin and in-house scripts (R Studio), and these data were used to calculate average migratory velocity according to the definition of Meyjering (19) during the observation period.

Statistical Analysis

All statistical analyses were performed using GraphPad Prism. Mann-Whitney U tests, Kruskal-Wallis tests followed by Dunn's *post hoc* tests, and paired Wilcoxon tests were used as appropriate; the test performed is noted in the figure legends. All p-values are presented as exact values with * indicated as follows: * p<0.05; ** p<0.01; *** p<0.001; and **** p<0.0001.

Data Availability

The data that support the findings of this study are available from the corresponding author upon reasonable request.

RESULTS

In-Depth Characterization of CD4 T Cell Subsets in Teriflunomide-Treated Patients With RRMS Shows No Impact After DHODH Inhibition

Using high-dimensional flow cytometry, we investigated the impact of DHODH inhibition in patients with RRMS before and 12 months posttreatment. The clinical characteristics of the patients are depicted in **Table 1**. We first focused on major lymphocyte populations (**Figure 1A**). The frequencies of leukocytes among B lymphocytes, NK CD56 cells, TCRγδ T cells and TCRαβ CD4 T cells were similar before and after teriflunomide treatment. Interestingly, a significant decrease in TCRαβ CD8 T cells was observed in patients with RRMS 12 months posttreatment (**Figure 1A**), resulting in an increase in the ratio of CD4/CD8 TCRαβ T cells (**Figure 1A**). We then applied high-dimensional flow cytometric analysis to investigate the CD4 T cell subsets. The CD4 T cell regulatory compartment was not impacted by DHODH inhibition, as shown by the similar frequency at baseline and 12 months posttreatment of CD4 regulatory T cells (T_{REGS}; CD25^{high}CD127^{low}), memory CD45RA⁻CD4 T_{REGS}, naïve CD45RA⁺CD4 T_{REGS} and follicular

CXCR5⁺CD4 T_{REGS} (**Figures 1B, C**). The expression of functional markers of CD4 T_{REGS} was also not impacted by DHODH inhibition, as the expression of regulatory associated molecules by CD4 T_{REG}, such as CTLA-4, LAG-3, and ectonucleotidases CD39 and CD73 CD4 T_{REG} (20), was similar before and 12 months post treatment (**Figure 1C**). To gain more insights into the T helper (T_H) and T follicular helper (T_{FH}) CD4 T cells, we applied global high-dimensional mapping of markers (CCR6, CXCR3, CCR4, CXCR5, CD161 and CD28) related to T_{FH}, T_{H1}, T_{H2}, T_{H17}, T_{H17.1}, T_{H22} T_{H9} and cytotoxic CD4 T cells [identified as described in a consensus paper (21)]. An optimized t-distributed stochastic neighbor embedding (opt-SNE) representation (22) of the data highlighted 12 major populations that were identified by FlowSOM clustering and the comparison of marker expression (**Figure 1D**). The opt-SNE representation of non-naïve CD4 T cells of patients at M00 was similar to that of patients 12 months posttreatment (**Figure 1E**) and was also evidenced by the analysis of the frequency of T_H and T_{FH} CD4 T cell clusters (**Figure 1F**). The cytokine profiles (T_{H1}, IFNγ, TNFα; T_{H2}, IL-13; T_{H17}, IL-17; and T_{REGS}, IL-10) produced by TCRαβ CD4 T cells (**Figure 1G**) and the proliferation of non-naïve TCRαβ CD4 T cells, T_{FH} cells and T_{REGS} (% of KI-67⁺; **Figure 1H**) confirmed the lack of impact of DHODH inhibition on the CD4 T compartment. Collectively, the longitudinal immune monitoring of patients with RRMS showed that DHODH inhibition selectively impacts the CD8 T cell compartment.

Teriflunomide Specifically Reduces the Proliferation and Immune Function of CD8 T Cells in Patients With RRMS

Seven major CD8 T cell populations were examined by using the combination of CD45RA, CD27, CCR7, and CD28 cell surface markers to define naïve (CD45RA⁺CD27⁺CCR7⁺CD28⁺), TEMRA (CD45RA⁺CD27⁻CCR7⁻CD28⁻), early-like effector memory (CD45RA⁻CD27⁻CCR7⁻CD28⁺), effector RA- [CD45RA⁻CD27⁻CCR7⁻CD28⁻ (TE RA⁻)], early memory [CD45RA⁻CD27⁺CCR7⁻CD28⁺ (early)], intermediate memory [CD45RA⁻CD27⁺CCR7⁻CD28⁻ (intermediate)], and central memory [CD45RA⁻CD27⁺CCR7⁺CD28⁺ (CM)] (**Figure 2A**) CD8 T cells [as described in a consensus paper (21)]. A nonsignificant increase in naïve CD8 T cells and a nonsignificant decrease in early CD8 T cells were observed in patients with RRMS 12 months posttreatment (**Figure 2A**). We then applied global high-dimensional mapping of the 27-parameter flow cytometry data to gain more insights into non-naïve αβ CD8 T cells. The opt-SNE representation of the data highlighted 20 populations that were identified by FlowSOM clustering and the comparison of marker expression (**Figure 2B**). The phenotype of the 20 populations at baseline was highly similar to those at 12 months posttreatment, as shown by the proximity of the 20 clusters after unsupervised clustering (**Figure 2B**). The opt-SNE representation of non-naïve CD8 T cells of patients at M00 was similar to that of patients at 12 months posttreatment (**Figure 2C**) and was shown by the analysis of the frequency of the 20 clusters of CD8 T cells (**Figure 2C**).

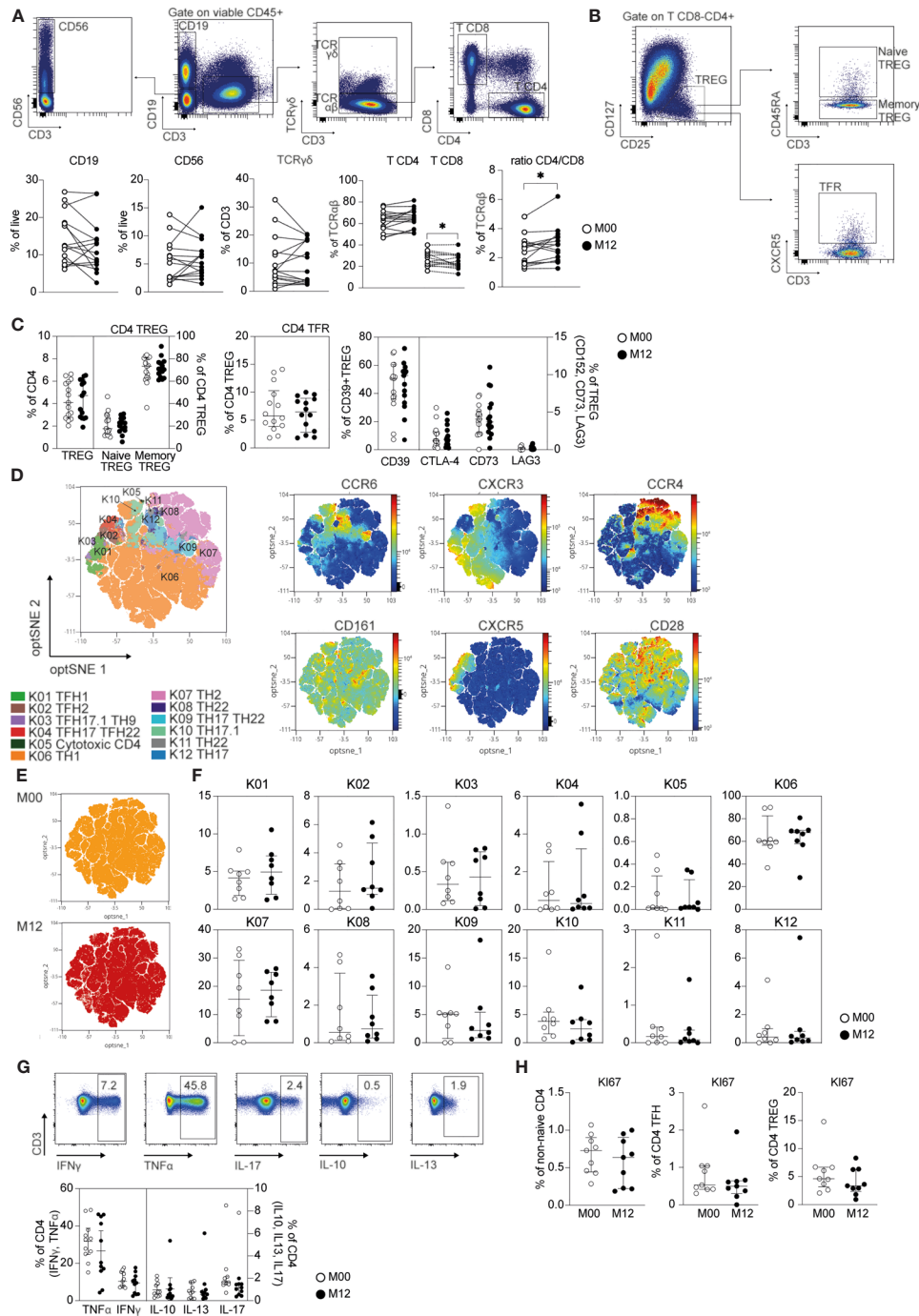


FIGURE 1 | CD4 and CD8 T cell changes in teriflunomide-treated patients with RRMS. **(A)** Main immune cell populations in patients with RRMS at baseline (white) or 12 months post teriflunomide treatment (black; n=15). The gating strategy is shown after exclusion of dead cells, doublets and CD45⁻ cells (B cells, CD19⁺CD3⁻CD56⁻; NK, CD56⁺CD19⁻CD3⁻; γδ T cells, CD19⁻CD56⁺CD3⁺TCRγδ⁺; αβ CD4 T cells, CD19⁻CD56⁻CD3⁺TCRγδ⁺CD8⁻CD4⁺; αβ CD8 T cells, CD19⁻CD56⁻CD3⁺TCRγδ⁺CD8⁺CD4⁻). **(B, C)** Frequency of CD4 T_{REG} and CD4 T_{REG} subsets in patients with RRMS at baseline (white) or 12 months post-teriflunomide treatment (black; n=15). The gating strategy is shown after initial gating on CD19⁻CD56⁻CD3⁺TCRγδ⁺CD8⁻CD4⁺ (T_{REG}S, CD25^{high}CD127^{low}; naive T_{REG}S, CD25^{high}CD127^{low}CD45RA⁺; memory T_{REG}S, CD25^{high}CD127^{low}CD45RA⁻; T_{FH}S, CD25^{high}CD127^{low}CXCR5⁺). **(D)** optSNE projection of non-naive αβ CD4 T cell clusters identified by FlowSOM metaclustering. optSNE projections of the expression of the indicated proteins are shown. **(E)** Global optSNE projection of non-naive αβ CD4 T cells for all participants pooled, with non-naive αβ CD4 T cells of patients with RRMS at M00 and M12 post-teriflunomide treatment concatenated and overlaid. **(F)** Percentage of non-naive αβ CD4 T cells from each timepoint in each FlowSOM cluster. **(G)** T_H1 cell (IFN_γ, TNF_α), T_H2 cell (IL-4, IL-13), T_{REG} (IL-10) and T_H17 cell (IL-17) cytokine production by CD4 T cells in patients with RRMS at M00 (white) and M12 post-teriflunomide treatment (black) after polyclonal restimulation. **(H)** Ki67 expression in non-naive αβ CD4 T cells, T_{FH} cells (non-naive αβ CD4 CXCR5⁺) and CD4 T_{REG}s. **(A, C, E-H)** Each dot represents a unique patient, and the median and interquartile ranges (IQRs) are shown. Significance was determined by unpaired Mann-Whitney U or paired Wilcoxon test. *p < 0.05.

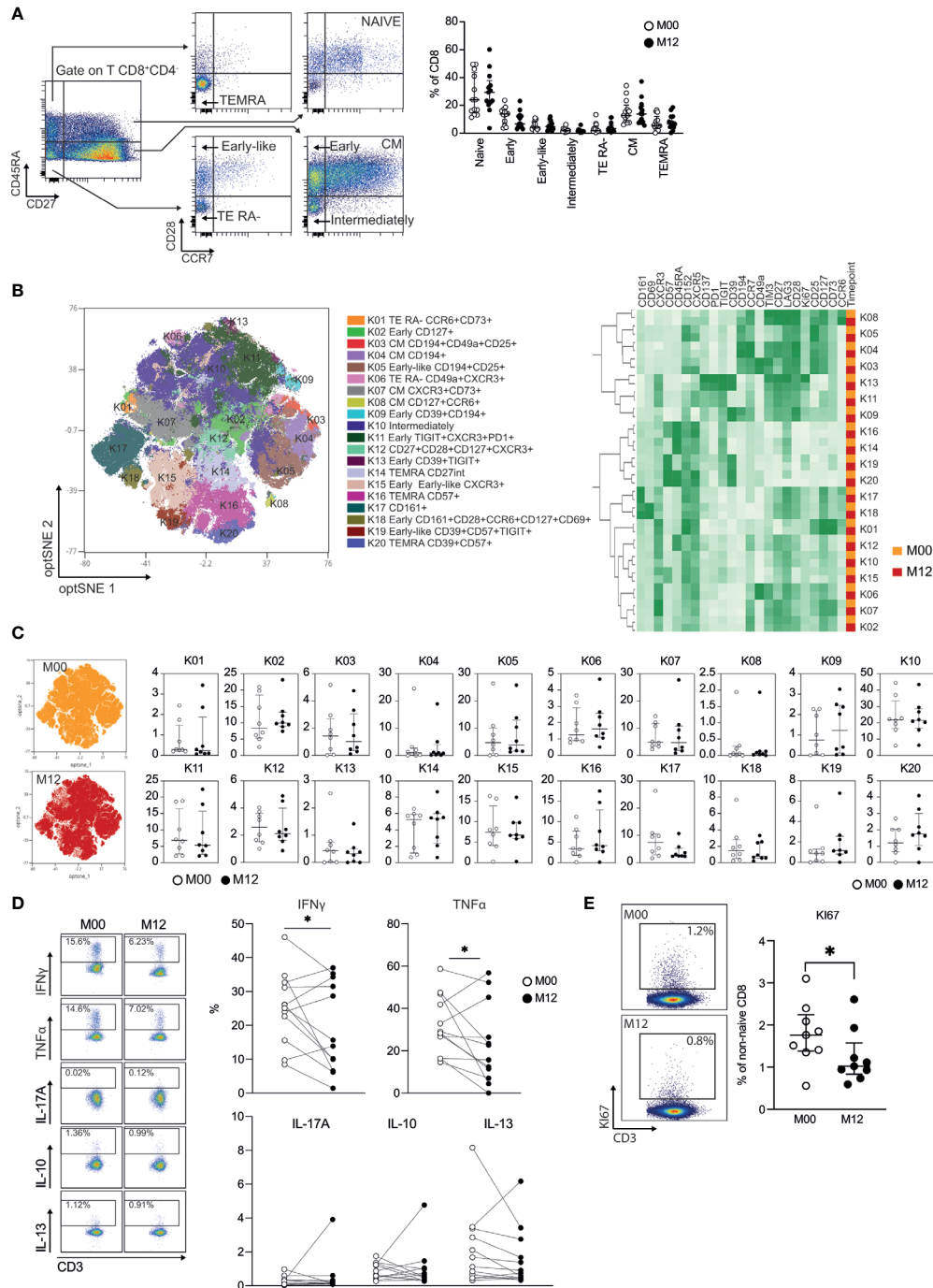


FIGURE 2 | Teriflunomide specifically reduces the proliferation and immune function of CD8 T cells in patients with RRMS. **(A)** Frequency of CD8 T cell subsets in patients with RRMS at baseline (white) or 12 months post-teriflunomide treatment (black; n=13). The gating strategy is shown after initial gating of CD19⁺CD56⁻CD3⁺TCR γ δ ⁺CD8⁺CD4⁻ cells (TEMRA, CD45RA⁺CD27⁺CCR7⁺CD28⁺; NAïVE, CD45RA⁺CD27⁺CCR7⁺CD28⁺; early-like, CD45RA⁺CD27⁺CCR7⁺CD28⁺; EM RA-, CD45RA⁺CD27⁺CCR7⁺CD28⁺; early, CD45RA⁺CD27⁺CCR7⁺CD28⁺; intermediately, CD45RA⁺CD27⁺CCR7⁺CD28⁺; CM, CD45RA⁺CD27⁺CCR7⁺CD28⁺). **(B)** optSNE projection of non-naïve $\alpha\beta$ CD8 T cell clusters identified by FlowSOM metaclustering (left) and mean fluorescence intensity (MFI) as indicated (column-scaled z-scores) for the FlowSOM cluster (right). **(C)** Global optSNE projection of non-naïve $\alpha\beta$ CD8 T cells for all participants pooled, with non-naïve $\alpha\beta$ CD8 T cells of patients with RRMS at M00 (white) and M12 post-teriflunomide treatment (black) concatenated and overlaid. Percentage of non-naïve $\alpha\beta$ CD8 T cells from each timepoint in each FlowSOM cluster. **(D)** T_H1 cell (IFN γ , TNF α), T_H2 cell (IL-13), T_{REG} (IL-10) and T_H17 cell (IL-17) cytokine production by CD8 T cells of patients with RRMS at M00 (white) and M12 post-teriflunomide treatment (black) after polyclonal restimulation. **(E)** Ki67 expression in non-naïve $\alpha\beta$ CD8 T cells. **(A, C–E)** Each dot represents a unique patient, and the median and interquartile ranges (IQRs) are shown. Significance was determined by unpaired Mann-Whitney U or paired Wilcoxon test (*p < 0.05).

Interestingly, the secretion of the proinflammatory cytokines IFN γ and TNF α produced by CD8 T cells was reduced in patients 12 months posttreatment (**Figure 2D**). The impact of DHODH inhibition was restricted to the production of proinflammatory cytokines by CD8 T cells, as the frequencies of IL-10 and IL-13 were similar before and 12 months posttreatment (**Figure 2D**). The reduced production of proinflammatory cytokines was confirmed in an analysis focused on TEMRA and EM CD8 T cell subsets (**Supplementary Figure 1**). Finally, a lower frequency of KI-67⁺ CD8 T cells was observed 12 months posttreatment (**Figure 2E**). The susceptibility of CD8 T cells of patients with RRMS to DHODH inhibition was confirmed *in vitro*, as the proliferation of EM and TEMRA CD8 T cells in response to TCR and IL-15 stimulation was blunted by teriflunomide, and the inhibition of proliferation can be reversed by added uridine (**Supplementary Figure 2**). In summary, we demonstrate that DHODH inhibition in patients with RRMS was associated with a lower *in vivo* proliferation of CD8 T cells with reduced proinflammatory properties 12 months after treatment.

Teriflunomide Inhibits the Migration of EM and TEMRA CD8 T Cells of Patients With RRMS *In Vitro*

We next tested the impact of DHODH inhibition on the patrolling properties of EM and TEMRA CD8 T cells of with RRMS, two CD8 T cell subsets in which predominant T cell clones were notable among CNS lesions, CSF, and blood CD8⁺ T cells were found (15). The dynamic behavior of TEMRA and EM CD8 T cells on activated endothelial cells was tracked using live-cell imaging (**Figure 3**). This dynamic model of T cell interaction with the activated endothelium showed that the EM and TEMRA CD8 T cells of patients with RRMS exhibited similar patrolling

behavior (**Figure 3**). Interestingly, the inhibition of DHODH resulted in the immediate and prolonged arrest of the EM and TEMRA CD8 T cells of patients with RRMS, as shown by the significant decrease in their average migratory velocity (**Figure 3B**). Finally, we assessed whether prolonged *in vivo* exposure to DHODH inhibition impacts the migratory properties of EM and TEMRA CD8 T cells of patients with RRMS. A nonsignificant decrease in the migratory velocity of the EM CD8 T cells was observed in the longitudinal follow-up of patients with RRMS 12 months after treatment (**Figure 3C**), whereas the velocity of the TEMRA CD8 T cells was not different before and 12 months posttreatment. Taken together, these results highlight that DHODH inhibition not only impacted the immune function of CD8 T cell subsets but also limited their migratory features.

Metabolic Characterization of EM and TEMRA CD8 T Cells in Patients With RRMS

As DHODH has been shown to interfere with components of the electron transport chain, we wondered whether the high and selective susceptibility of CD8 T cells of patients with RRMS might be linked to impaired CD8 T cell energy metabolism. In the steady state, all CD8 T cell subsets (naïve, EM and TEMRA T cells) in patients with RRMS exhibited a higher mitochondrial mass than those of HVs (**Figure 4A**) with a higher energy activation in mitochondria, as shown by the mitochondrial membrane potential (MMP) measured using a voltage-dependent MitoTracker probe (**Figure 4B**). The absence of mitochondrial defects in CD8 T cell subsets in patients with RRMS was confirmed using a Seahorse assay. Basal respiration

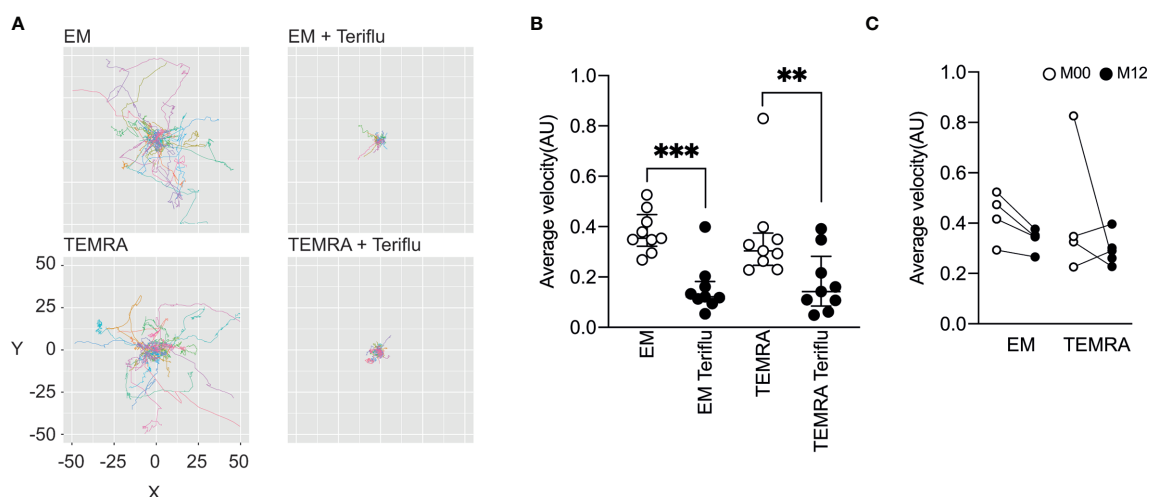


FIGURE 3 | Teriflunomide inhibits the migration of EM and TEMRA CD8 T cells in patients with RRMS. **(A, B)** Migration of Fura-2-labeled CD8 T cell subsets of patients with RRMS onto TNF α (100 U/ml, O/N)-treated HDMEC monolayers and, as indicated, when teriflunomide (100 μ M) was added 15' after the initial recording. Paths of individual cells were aligned to their origins at x=y=0 **(A)**, and the average velocity **(B)** of CD8 T cell subsets is shown. **(C)** Migration of Fura-2-labeled CD8 T cell subsets of patients with RRMS at M00 (white) and at M12 (black) post-teriflunomide treatment onto TNF α (100 U/ml, O/N)-treated HDMEC monolayers. Average velocity of CD8 T cell subsets is shown. **(B, C)** Each dot represents a unique patient, and the median and interquartile ranges (IQRs) are shown. Significance was determined by unpaired Mann-Whitney U test (**p < 0.01; ***p < 0.001).

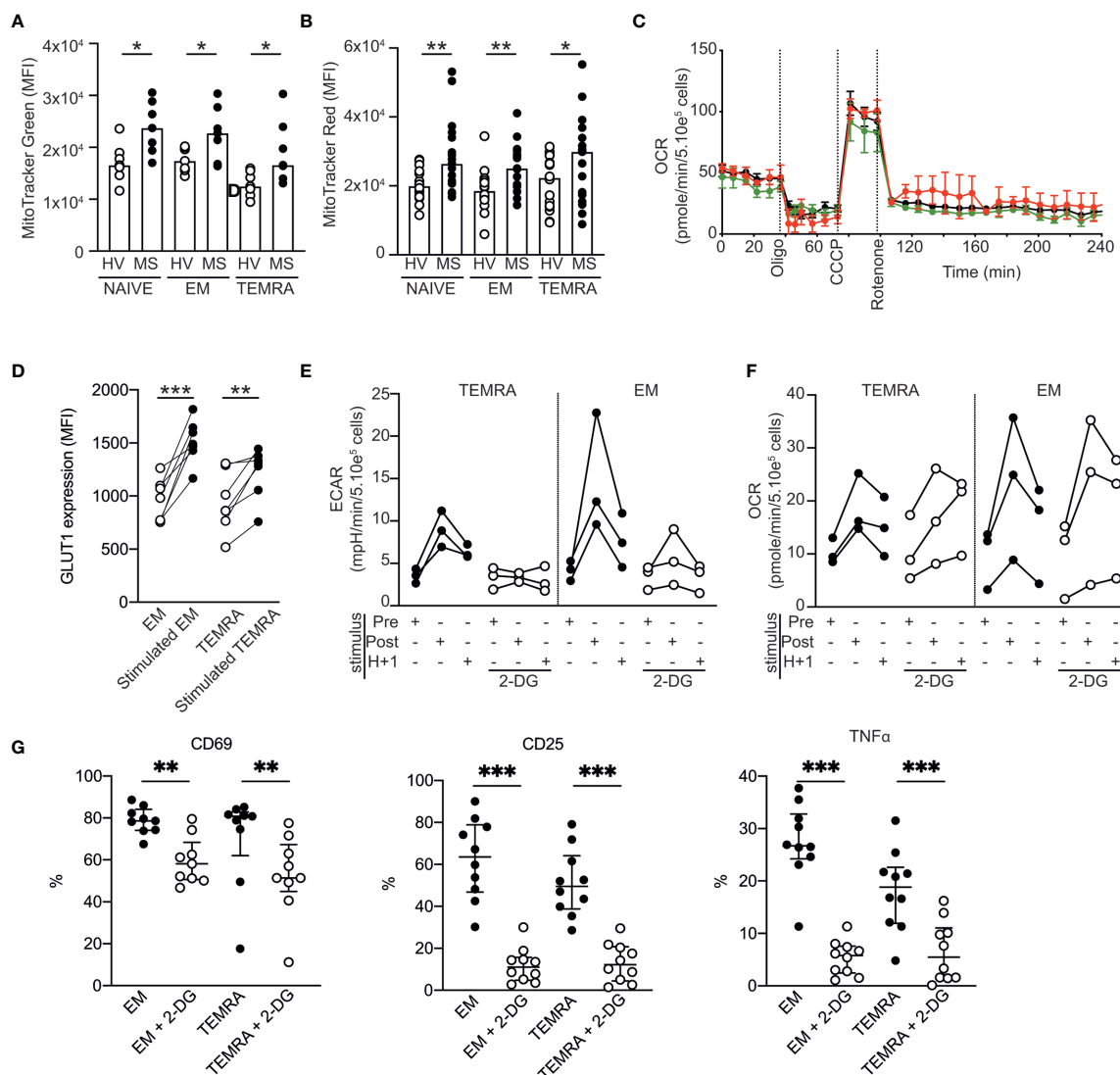


FIGURE 4 | Metabolic characterization of CD8 T cell subsets in patients with RRMS. **(A, B)** Mitochondrial load **(A)** and mitochondrial membrane potential **(B)** of CD8 T cell subsets of HVs and patients with RRMS assessed according to the mean fluorescence intensity of MitoTracker green and red, respectively. **(C)** Oxygen consumption rate (OCR) of purified CD8 T cell subsets as measured by Seahorse technology before and after sequential addition of metabolic stress-inducing drugs. **(D)** Expression of GLUT-1 by EM and TEMRA CD8 T cells of patients with RRMS upon overnight stimulation with plate-bound anti-CD3. **(E, F)** Extracellular acidification rate [ECAR; **(E)**] and OCR **(F)** of EM and TEMRA CD8 T cells of patients with RRMS before and after polyclonal stimulation in the absence or in the presence of the glycolysis inhibitor 2-DG. **(G)** Expression of activation markers (CD69 and CD25) and proinflammatory cytokines (TNF α) in EM and TEMRA CD8 T cells of patients with RRMS after overnight stimulation with plate-bound anti-CD3 and IL-15 in the presence of medium control or 2-DG. **(A, B, D-G)** Each dot represents a unique patient, and the median and interquartile ranges (IQRs) are shown. Significance was determined by unpaired Mann-Whitney U or paired Wilcoxon test (* $p < 0.05$; ** $p < 0.01$; *** $p < 0.001$). **(C)** Representative OCR profile from one out of 5 patients with RRMS.

was similar across the different CD8 T cell subsets (**Figure 4C**), and as expected, the injection of oligomycin, an inhibitor of ATP synthase, induced a rapid decrease in the oxygen consumption rate (**Figure 4C**), demonstrating the mitochondrial coupling efficiency. Finally, the protonophore CCCP resulted in an increase in OCR in all CD8 T cell subsets (**Figure 4C**). Collectively, these results showed that CD8 T cell subsets of patients with RRMS exhibited well-functioning mitochondria under steady state conditions.

The ability to rapidly switch to glycolysis-based metabolism upon stimulation is a hallmark of memory CD8 T cells (23). We showed that, upon stimulation, EM and TEMRA CD8 T cell subsets of patients with RRMS exhibited modified nutrient uptake and metabolism to satisfy their bioenergetic needs, as shown by the increase in their ability to take up glucose (increased expression of glucose transporter 1 GLUT1; **Figure 4D**) and in the extracellular acidification rate (ECAR; an indicator of glycolysis; **Figure 4E**) and OCR within minutes following polyclonal stimulation (**Figure 4F**). As expected, the

addition of 2-deoxyglucose (2-DG), which blocks the first step of the glycolytic pathway, prevented both the immediate and sustained increases in the ECAR while not increasing the OCR (Figures 4E, F). The impact of 2DG on glycolysis inhibition resulted in reduced activation of the EM and TEMRA CD8 T cell subsets of patients with RRMS, which showed lower expression of the early activation marker CD69 and the high-affinity IL-2 receptor CD25 and lower TNF α production (Figure 4G). Collectively, these data showed the ability of EM and TEMRA CD8 T cell subsets of patients with RRMS to adapt their metabolism to engage their effector function, and therefore, the selective susceptibility of CD8 T cells of patients with RRMS to DHODH inhibition was not related to impaired CD8 T cell energy metabolism.

DISCUSSION

Teriflunomide has been shown to be an effective therapy to treat patients with MS in placebo-controlled phase 3 trials [TEMSo (1) and TOWER (2)]. Recently, we confirmed these results in real-life settings, and we reported that teriflunomide and dimethyl fumarate have similar clinical effectiveness after 2 years of treatment of a large number of patients with RRMS (24). The underlying mechanism contributing to the efficacy of DHODH inhibition remains only partially elucidated. Here, using high-dimensional approaches, we demonstrate that patients with RRMS treated with teriflunomide exhibited a selective alteration of the CD8 T cell compartment as characterized by low homeostatic proliferation of CD8 T cells, low production of proinflammatory cytokines by memory CD8 T cells and decreased migratory velocity of memory CD8 T cells. Interestingly, B cell subsets and CD4 Treg, CD4 T_{FH} and CD4 T_H cell subsets were not impacted by 12 months of teriflunomide treatment.

It has been established that CD8 T cells play major roles in the pathogenesis of MS, as the clonal composition of T cells infiltrating active lesions shows predominant CD8 T cell infiltration (14, 15, 25–29). Expanded CD8 T cell clones have also been found in paired analysis of blood, cerebrospinal fluid (CSF) and active white matter lesions (14, 15, 27). CD8 T cells identified in white matter lesions were reported to show effector memory phenotypes (15, 27) with chronic activation (expressing CD95L and granzyme B) (27), with a high frequency of the CD8 T cells expressing coinhibitory receptors (TIM3 and PD1) (27) or a tissue-resident memory phenotype (29, 30). Indeed, single-cell RNA sequencing of cells infiltrating the cerebrospinal fluid (CSF) in patients with MS revealed that CD8 T cells were the main contributor of clonally expanded T cells with an activated tissue-resident memory phenotype (29), an observation in agreement with the *in situ* staining of CD8 T cells of white matter active lesions reported by Machado-Santos et al. (30) CNS-infiltrating CD8 T cell clones have also been detected in the CSF and in the blood, suggesting that uncommitted CD8 memory precursor T cells migrate from the periphery to the CSF and the CNS, where they acquire a tissue-resident memory phenotype. Alternatively,

as shown for mouse epidermal resident memory CD8 T cells (31), naïve CD8 T cells can be primed for tissue residency. The selective alteration of CD8 T cell function reported herein strengthens previous findings showing that CD8 T cells are involved in MS and may partially explain the therapeutic efficacy of teriflunomide. An obvious limitation of our study is the small sample size. Nevertheless, we circumvented the confounding factor of treatment by systematically analyzing the effects of MS patient treatment through a longitudinal approach and by using paired analysis of samples (each patient being his own reference control).

Whether autoreactive T cells are recruited to the CNS remains a key unanswered question. Nevertheless, in this study, we showed that *in vitro* inhibition of DHODH alters the migratory properties of CD8 T cells in patients with RRMS, and interestingly, the velocity of CD8 T cell subsets of these patients was lower after 12 months of treatment with teriflunomide. These results suggest an additional mechanism of action of teriflunomide by which it limits the ability of memory CD8 T cells to infiltrate the CSF and CNS. This limitation of migratory fitness of memory CD8 T cells induced by teriflunomide has been previously suggested on the basis of the inhibition of integrin LFA-1 avidity after *in vitro* treatment with teriflunomide (32).

Teriflunomide has been shown to induce a modest but stable lymphopenia in patients with MS and the meta-analysis of patients enrolled in the TEMSo (1) and TOWER (2) phase 3 clinical trials show a mean decrease in leukocyte counts of 15% from baseline (4). Previous longitudinal studies have shown a stability in the composition of the CD4 and CD8 T subsets in patients RRMS analyzed 6 months after teriflunomide treatment (9, 10). Our findings confirm these results in MS patients after one-year of treatment with teriflunomide with no significant modification of the frequency of the CD4/CD8 T cell subsets analyzed with our comprehensive spectral flow cytometry panel. The current understanding of the mechanism of action of teriflunomide suggests that it can inhibit the proliferation of metabolically active T cells, a concept that has been further supported by the demonstration that high-affinity T cells are more susceptible to DHODH inhibition (10). No direct impact on cell survival has been reported (3). Based on surrogate markers of CD4 TH cells (i.e. chemokine receptors), a preferential reduction in TH1 CD4 T cells was reported while no modification in the other TH CD4 was observed including no impact on TH17 CD4 subsets (10). In the current study and based on the profiling of cytokines production by CD4 T cells, we also reported a trend in a lower secretion of TNF α and IFN γ by CD4 T cells after teriflunomide treatment (Figure 1G). We now also report that the *in vivo* proliferation of CD8 T cells and the production of pro-inflammatory cytokines by CD8 T cells are lower after treatment with teriflunomide. The impact of teriflunomide on CD8 T cells may suggest that, after treatment, MS patients may have a lower response upon viral infection. Nevertheless, published reports of large cohort of patients treated with teriflunomide failed to demonstrate any increase in opportunistic infections. The incidence of serious

infections was not different between placebo-treated patients and Teriflunomide-treated patients (33) and the long-term follow-up of patients of the TEMSO studies did not evidence any serious opportunistic infections (33, 34). The ability to mount protective vaccine responses to recall antigens is preserved in MS patients treated with Teriflunomide (35). Finally, in the context of the current SARS-CoV-2 pandemic, case reports have shown that the continuation of Teriflunomide could be continued for MS patients and was not associated with negative outcome (36–42).

Although few reports have characterized immune metabolism in patients with autoimmune diseases such as systemic lupus erythematosus (43) or rheumatoid arthritis (44), the concept of a disease-specific signature of immune metabolism seems to prevail. In patients with MS, CD4 T cell metabolism has been shown to differ between patients with primary progressive MS (PPMS) and those with secondary progressive (SPMS) MS (45). Naïve and EM CD4 T cells of patients with PPMS have been shown to exhibit lower mitochondrial respiration, lower glycolytic rates and accumulation of disorganized mitochondria than CD4 T cells of SPMS patients (45). In contrast, oxidative phosphorylation and glycolysis in CD4 T cells have been found to be increased in patients with active RRMS compared to clinically stable patients and healthy controls (10). Here, we showed that CD8 T cell subsets (EM and TEMRA) exhibited an increased number of functional mitochondria in patients with RRMS compared to healthy controls. The fitness of the metabolic processes of EM and TEMRA CD8 T cells in patients with RRMS was confirmed by increased OCRs and ECARs in these cells upon stimulation and the ability of 2-DG treatment to blunt glycolysis and thus prevent an immune response. The upregulation of aerobic glycolysis upon pro-inflammatory stimulation is a shared characteristic seen in activated B cells, CD4 TH1/TH17 cells, CD8 T cells, educated NK cells and activated M1 macrophages. As a consequence, the interference of glycolysis is expected to control the pro-inflammatory response in patients, including in patients with MS. The selectivity of targeting metabolic processes is expected to be achieved by the high metabolic demands of target cells whereas other immune cells could be spared reducing unwanted side effects (46, 47).

Taken together, these findings strengthen the concept of disease-specific alteration of T cell immune metabolism in autoimmune diseases.

DATA AVAILABILITY STATEMENT

The raw data supporting the conclusions of this article will be made available by the authors, without undue reservation.

ETHICS STATEMENT

The studies involving human participants were reviewed and approved by the University Hospital Committee and the Committee for the Protection of Patients from Biological Risks. The patients/participants provided their written informed consent to participate in this study.

AUTHOR CONTRIBUTIONS

GT: Methodology, Visualization, Validation, Formal analysis, Writing – Original draft. MC: Methodology, Formal analysis. AG: Resources, Data Curation, Formal analysis. JM: Resources. SW: Resources, Data Curation. CP, Methodology, Validation. SB: Conceptualization, Supervision, Writing – Review & Editing. DL: Conceptualization, Funding acquisition, Data Curation, Writing – Review & Editing. ND: Conceptualization, Funding acquisition, Software, Validation, Visualization, Formal analysis, Writing – Original draft, Writing – Review & Editing. All authors contributed to the article and approved the submitted version.

FUNDING

This work was supported by a Genzyme Research grant and also partially supported by a grant from the LabEX IGO program supported by the National Research Agency *via* the “Investment into the Future” program (ANR-11-LABX-0016-01) and by the Public Investment Bank, also known as BPI France in the framework of the “Investment for the Future” programme (Programme d’Investissements d’Avenir). This work was also supported by the FP7 VISICORT project, which has received funding from the European Union’s Seventh Framework Programme for research, technological development and demonstration under grant agreement 602470.

ACKNOWLEDGMENTS

The authors would like to thank the patients for their participation in the study and the Cellular and Tissular Imaging Core Facility of Nantes University (MicroPICell) for their excellent technical support.

SUPPLEMENTARY MATERIAL

The Supplementary Material for this article can be found online at: <https://www.frontiersin.org/articles/10.3389/fimmu.2021.730342/full#supplementary-material>

Supplementary Figure 1 | Hyporesponsiveness of EM and TEMRA CD8 T cells of teriflunomidetreated patients with RRMS. Production of IFN γ and TNF α by CD8 EM and TEMRA cells of patients with RRMS at M00 (white) and at M12 (black) post-teriflunomide treatment. Each dot represents a unique patient, and the median and interquartile ranges (IQRs) are shown. Significance was determined by paired Wilcoxon test (** $p < 0.01$).

Supplementary Figure 2 | Teriflunomide inhibits the proliferation of EM and TEMRA CD8 T cells of patients with RRMS. Percentage of CPDeFluor450low after stimulation of CD8 T cells of patients with RRMS with plate-bound anti-CD3 and IL15 in the presence of medium control or teriflunomide (100 μ M) and, when indicated, uridine (50 μ M). Each dot represents a unique patient, and the median is shown. Significance was determined by unpaired Mann-Whitney U test (** $p < 0.01$).

REFERENCES

- O'Connor P, Wolinsky JS, Confavreux C, Comi G, Kappos L, Olsson TP, et al. Randomized Trial of Oral Teriflunomide for Relapsing Multiple Sclerosis. *N. Engl J Med* (2011) 365:1293–303. doi: 10.1056/nejmoa1014656
- Confavreux C, O'Connor P, Comi G, Freedman MS, Miller AE, Olsson TP, et al. Oral Teriflunomide for Patients With Relapsing Multiple Sclerosis (TOWER): A Randomised, Double-Blind, Placebo-Controlled, Phase 3 Trial. *Lancet Neurol* (2014) 13:247–56. doi: 10.1016/s1474-4422(13)70308-9
- Li L, Liu J, Delohery T, Zhang D, Arendt C, Jones C. The Effects of Teriflunomide on Lymphocyte Subpopulations in Human Peripheral Blood Mononuclear Cells *In Vitro*. *J Neuroimmunol* (2013) 265:82–90. doi: 10.1016/j.jneuroim.2013.10.003
- Bar-Or A, Pachner A, Menguy-Vacheron F, Kaplan J, Wiendl H. Teriflunomide and Its Mechanism of Action in Multiple Sclerosis. *Drugs* (2014) 74:659–74. doi: 10.1007/s40265-014-0212-x
- Cherwinski HM, Cohn RG, Cheung P, Webster DJ, Xu YZ, Caulfield JP, et al. The Immunosuppressant Leflunomide Inhibits Lymphocyte Proliferation by Inhibiting Pyrimidine Biosynthesis. *J Pharmacol Exp Ther* (1995) 275:1043–9.
- Rückemann K, Fairbanks LD, Carrey EA, Hawrylowicz CM, Richards DF, Kirschbaum B, et al. Leflunomide Inhibits Pyrimidine De Novo Synthesis in Mitogen-Stimulated T-Lymphocytes From Healthy Humans*. *J Biol Chem* (1998) 273:21682–91. doi: 10.1074/jbc.273.34.21682
- O'Neill LAJ, Kishton RJ, Rathmell J. A Guide to Immunometabolism for Immunologists. *Nat Rev Immunol* (2016) 16:553–565. doi: 10.1038/nri.2016.70
- Wang R, Green DR. Metabolic Reprogramming and Metabolic Dependency in T Cells. *Immunol Rev* (2012) 249:14–26. doi: 10.1111/j.1600-065x.2012.01155.x
- Medina S, Maza SS de la, Villarrubia N, Álvarez-Lafuente R, Costa-Frossard L, Arroyo R, et al. Teriflunomide Induces a Tolerogenic Bias in Blood Immune Cells of MS Patients. *Ann Clin Transl Neur* (2019) 6:355–63. doi: 10.1002/acn3.711
- Klotz L, Eschborn M, Lindner M, Liebmann M, Herold M, Janoschka C, et al. Teriflunomide Treatment for Multiple Sclerosis Modulates T Cell Mitochondrial Respiration With Affinity-Dependent Effects. *Sci Transl Med* (2019) 11:eaa05563. doi: 10.1126/scitranslmed.aao5563
- Krishnamoorthy G, Wekerle H. EAE: An Immunologist's Magic Eye. *Eur J Immunol* (2009) 39:2031–5. doi: 10.1002/eji.200939568
- Siewert K, Malotka J, Kawakami N, Wekerle H, Hohlfeld R, Dornmair K. Unbiased Identification of Target Antigens of CD8+ T Cells With Combinatorial Libraries Coding for Short Peptides. *Nat Med* (2012) 18:824–8. doi: 10.1038/nm.2720
- Neumann H, Medana IM, Bauer J, Lassmann H. Cytotoxic T Lymphocytes in Autoimmune and Degenerative CNS Diseases. *Trends Neurosci* (2002) 25:313–9. doi: 10.1016/s0166-2236(02)02154-9
- Skulina C, Schmidt S, Dornmair K, Babbe H, Roers A, Rajewsky K, et al. Multiple Sclerosis: Brain-Infiltrating CD8+ T Cells Persist as Clonal Expansions in the Cerebrospinal Fluid and Blood. *Proc Natl Acad Sci USA* (2004) 101:2428–2433. doi: 10.1073/pnas.0308689100
- Salou M, Garcia A, Michel L, Gainche-Salmon A, Loussouarn D, Nicol B, et al. Expanded CD8 T-Cell Sharing Between Periphery and CNS in Multiple Sclerosis. *Ann Clin Transl Neur* (2015) 2:609–22. doi: 10.1002/acn3.199
- Meskas J, Wang S, Brinkman R. Flowcut — An R Package for Precise and Accurate Automated Removal of Outlier Events and Flagging of Files Based on Time Versus Fluorescence Analysis. *Biorxiv* (2020). doi: 10.1101/2020.04.23.058545. 2020.04.23.058545.
- Gassen SV, Callebaut B, Helden MJV, Lambrecht BN, Demeester P, Dhaene T, et al. FlowSOM: Using Self-Organizing Maps for Visualization and Interpretation of Cytometry Data. *Cytom Part A* (2015) 87:636–45. doi: 10.1002/cyto.a.22625
- Swerlicka RA, Lawley TJ. Role of Microvascular Endothelial Cells in Inflammation. *J Invest Dermatol* (1993) 100:111S–5S. doi: 10.1111/1523-1747.ep12356595
- Meijering E, Dzyubachyk O, Smal I. Chapter Nine Methods for Cell and Particle Tracking. *Methods Enzymol* (2012) 504:183–200. doi: 10.1016/b978-0-12-391857-4.00009-4
- Deaglio S, Dwyer KM, Gao W, Friedman D, Usheva A, Erat A, et al. Adenosine Generation Catalyzed by CD39 and CD73 Expressed on Regulatory T Cells Mediates Immune Suppression. *J Exp Med* (2007) 204:1257–65. doi: 10.1084/jem.20062512
- Cossarizza A, Chang H, Radbruch A, ACS A, Adam D, Adam-Klages S, et al. Guidelines for the Use of Flow Cytometry and Cell Sorting in Immunological Studies (Second Edition). *Eur J Immunol* (2019) 49:1457–973. doi: 10.1002/eji.201970107
- Belkina AC, Ciccolella CO, Anno R, Halpert R, Spidlen J, Snyder-Cappione JE. Automated Optimized Parameters for T-Distributed Stochastic Neighbor Embedding Improve Visualization and Analysis of Large Datasets. *Nat Commun* (2019) 10:5415. doi: 10.1038/s41467-019-13055-y
- Gubser PM, Bantug GR, Razik L, Fischer M, Dimeloe S, Hoenger G, et al. Rapid Effector Function of Memory CD8+ T Cells Requires an Immediate-Early Glycolytic Switch. *Nat Immunol* (2013) 14:1064–72. doi: 10.1038/ni.2687
- Laplaud D-A, Casey R, Barbin L, Debouverie M, Sèze JD, Brassat D, et al. Comparative Effectiveness of Teriflunomide vs Dimethyl Fumarate in Multiple Sclerosis. *Neurology* (2019) 93:e635–46. doi: 10.1212/wnl.0000000000007938
- Babbe H, Roers A, Waisman A, Lassmann H, Goebels N, Hohlfeld R, et al. Clonal Expansions of CD8+ T Cells Dominate the T Cell Infiltrate in Active Multiple Sclerosis Lesions as Shown by Micromanipulation and Single Cell Polymerase Chain Reaction. *J Exp Med* (2000) 192:393–404. doi: 10.1084/jem.192.3.393
- Junker A, Ivanidze J, Malotka J, Eiglmeier I, Lassmann H, Wekerle H, et al. Multiple Sclerosis: T-Cell Receptor Expression in Distinct Brain Regions. *Brain* (2007) 130:2789–99. doi: 10.1093/brain/awm214
- Nierop GPv, Luijck MMv, Michels SS, Melief M-J, Janssen M, Langerak AW, et al. Phenotypic and Functional Characterization of T Cells in White Matter Lesions of Multiple Sclerosis Patients. *Acta Neuropathol* (2017) 134:383–401. doi: 10.1007/s00401-017-1744-4
- Held K, Bhonsle-Deeng L, Siewert K, Sato W, Beltrán E, Schmidt S, et al. T-Cell Receptors From Multiple Sclerosis Brain Lesions Show MAIT Cell-Related Features. *Neurol Neuroimmunol Neuroinflamm* (2015) 2:NA. doi: 10.1212/nxi.0000000000000107
- Beltrán E, Gerdes LA, Hansen J, Flierl-Hecht A, Krebs S, Blum H, et al. Early Adaptive Immune Activation Detected in Monozygotic Twins With Prodromal Multiple Sclerosis. *J Clin Invest* (2019) 129:4758–68. doi: 10.1172/jci.128475
- Machado-Santos J, Saji E, Tröscher AR, Paunovic M, Liblau R, Gabrieli G, et al. The Compartmentalized Inflammatory Response in the Multiple Sclerosis Brain Is Composed of Tissue-Resident CD8+ T Lymphocytes and B Cells. *Brain* (2018) 141:2066–82. doi: 10.1093/brain/awy151
- Mani V, Bromley SK, Åijö T, Mora-Buch R, Carrizosa E, Warner RD, et al. Migratory DCs Activate TGF- β to Precondition Naïve CD8+ T Cells for Tissue-Resident Memory Fate. *Science* (2019) 366:eav5728. doi: 10.1126/science.aav5728
- Zeyda M, Poglitsch M, Geyeregger R, Smolen JS, Zlabinger GJ, Hörl WH, et al. Disruption of the Interaction of T Cells With Antigen-Presenting Cells by the Active Leflunomide Metabolite Teriflunomide: Involvement of Impaired Integrin Activation and Immunologic Synapse Formation. *Arthritis Rheumatism* (2005) 52:2730–9. doi: 10.1002/art.21255
- Singer B, Comi G, Miller A, Olsson T, Wolinsky J, Kappos L, et al. Frequency of Infections During Treatment With Teriflunomide: Pooled Data From Three Placebo-Controlled Teriflunomide Studies (P01.171). *Neurology* (2013) 80:P01.171–P01.171.
- Confavreux C, Li DK, Freedman MS, Truffinet P, Benzerdjeb H, Wang D, et al. Long-Term Follow-Up of a Phase 2 Study of Oral Teriflunomide in Relapsing Multiple Sclerosis: Safety and Efficacy Results Up to 8.5 Years. *Mult Scler J* (2012) 18:1278–89. doi: 10.1177/1352458512436594
- Bar-Or A, Freedman MS, Kremenutzky M, Menguy-Vacheron F, Bauer D, Jodl S, et al. Teriflunomide Effect on Immune Response to Influenza Vaccine in Patients With Multiple Sclerosis. *Neurology* (2013) 81:552–8. doi: 10.1212/wnl.0b013e31829e6fbf
- Capone F, Motolese F, Luce T, Rossi M, Magliozzi A, Lazzaro VD. COVID-19 in Teriflunomide-Treated Patients With Multiple Sclerosis: A Case Report and Literature Review. *Mult Scler Relat Dis* (2021) 48:102734. doi: 10.1016/j.msard.2020.102734

37. Luca B, Tommaso G, Bavaro DF, Laura M, Annalisa S, Gioacchino A, et al. Seroconversion and Indolent Course of COVID-19 in Patients With Multiple Sclerosis Treated With Fingolimod and Teriflunomide. *J Neurol Sci* (2020) 416:117011. doi: 10.1016/j.jns.2020.117011
38. Ciardi MR, Zingaropoli MA, Pasculli P, Perri V, Tartaglia M, Valeri S, et al. The Peripheral Blood Immune Cell Profile in a Teriflunomide-Treated Multiple Sclerosis Patient With COVID-19 Pneumonia. *J Neuroimmunol* (2020) 346:577323. doi: 10.1016/j.jneuroim.2020.577323
39. Maghzi AH, Houtchens MK, Preziosa P, Ionete C, Beretich BD, Stankiewicz JM, et al. COVID-19 in Teriflunomide-Treated Patients With Multiple Sclerosis. *J Neurol* (2020) 267:2790–6. doi: 10.1007/s00415-020-09944-8
40. Mantero V, Baroncini D, Balgera R, Guaschino C, Basilico P, Annovazzi P, et al. Mild COVID-19 Infection in a Group of Teriflunomide-Treated Patients With Multiple Sclerosis. *J Neurol* (2021) 268:2029–30. doi: 10.1007/s00415-020-10196-9
41. Möhn N, Saker F, Bonda V, Respondek G, Bachmann M, Stoll M, et al. Mild COVID-19 Symptoms Despite Treatment With Teriflunomide and High-Dose Methylprednisolone Due to Multiple Sclerosis Relapse. *J Neurol* (2020) 267:2803–5. doi: 10.1007/s00415-020-09921-1
42. Louapre C, Collongues N, Stankoff B, Giannesini C, Papeix C, Bensa C, et al. Clinical Characteristics and Outcomes in Patients With Coronavirus Disease 2019 and Multiple Sclerosis. *JAMA Neurol* (2020) 77(9):1079–88. doi: 10.1001/jamaneurol.2020.2581
43. Yin Y, Choi S-C, Xu Z, Perry DJ, Seay H, Croker BP, et al. Normalization of CD4+ T Cell Metabolism Reverses Lupus. *Sci Transl Med* (2015) 7:274ra18. doi: 10.1126/scitranslmed.aaa0835
44. Yang Z, Fujii H, Mohan SV, Goronzy JJ, Weyand CM. Phosphofructokinase Deficiency Impairs ATP Generation, Autophagy, and Redox Balance in Rheumatoid Arthritis T Cells. *J Exp Med* (2013) 210:2119–34. doi: 10.1084/jem.20130252
45. Biasi S, Simone AM, Bianchini E, Tartaro D, Pecorini S, Nasi M, et al. Mitochondrial Functionality and Metabolism in T Cells From Progressive Multiple Sclerosis Patients. *Eur J Immunol* (2019) 49:2204–21. doi: 10.1002/eji.201948223
46. Pålsson-McDermott EM, O'Neill LAJ. Targeting Immunometabolism as an Anti-Inflammatory Strategy. *Cell Res* (2020) 30:300–14. doi: 10.1038/s41422-020-0291-z
47. Degauque N, Brosseau C, Brouard S. Regulation of the Immune Response by the Inflammatory Metabolic Microenvironment in the Context of Allogeneic Transplantation. *Front Immunol* (2018) 9:1465. doi: 10.3389/fimmu.2018.01465

Conflict of Interest: DL has received consulting and lecturing fees, travel grants and unconditional research support from Biogen, Genzyme, Novartis, Merck, Roche, Sanofi, Medday, Teva Pharma and BMS. SW has received speaking honoraria and travel expense reimbursement for participation in scientific meetings and has participated in advisory boards in the past years with Alexion, Biogen, Merck, Novartis, Roche, Sanofi and Teva.

The remaining authors declare that the research was conducted in the absence of any commercial or financial relationships that could be construed as a potential conflict of interest.

Publisher's Note: All claims expressed in this article are solely those of the authors and do not necessarily represent those of their affiliated organizations, or those of the publisher, the editors and the reviewers. Any product that may be evaluated in this article, or claim that may be made by its manufacturer, is not guaranteed or endorsed by the publisher.

Copyright © 2021 Tilly, Cadoux, Garcia, Morille, Wiertlewski, Pecqueur, Brouard, Laplaud and Degauque. This is an open-access article distributed under the terms of the Creative Commons Attribution License (CC BY). The use, distribution or reproduction in other forums is permitted, provided the original author(s) and the copyright owner(s) are credited and that the original publication in this journal is cited, in accordance with accepted academic practice. No use, distribution or reproduction is permitted which does not comply with these terms.